Sensorless Position Control of Skewed Rotor Induction Machines Based on Multi Saliency Extraction

T.M. Wolbank
Department of Electrical Drives and Machines
Vienna University of Technology
Vienna, AUSTRIA
e-mail: thomas.wolbank@*tuwien.ac.at*

M.K. Metwally
Department of Electrical Drives and Machines
Vienna University of Technology
Vienna, AUSTRIA

Abstract-**This paper addresses sensorless position and torque control of induction machines around zero frequency using inherent saliencies of a skewed rotor machine. The estimation method employs transient excitation of voltage pulses to detect machine saliencies. The resulting signals from injection based sensorless control methods are composed of components caused by saturation, slotting, as well as inter-modulation effects. As multiple saliencies cause problems in tracking only a particular saliency, decoupling of the different signal components is applied via neural network. This leads to the estimation of both the rotor angle as well as the flux angle, which are used in combination with the stator and the rotor equations. Identifying the disturbances of the different signal components it is possible to establish an adaptive control signal merging to reduce disturbance based torque pulsations. The performance of the control is investigated at loaded operation and zero speed as well as zero fundamental frequency.**

I. INTRODUCTION

Most of the scientific and technical efforts performed over the past two decades on sensorless control of AC drives have moved from being purely a research topic to being widely used in different industrial applications. It is accepted that no single sensorless method is capable of controlling all types of machines, under all operating conditions. Back-emf based techniques have been shown to be capable of providing high performance, field-oriented control in the medium to high speed range. As the speed decreases, the parameter sensitivity of these methods becomes bigger, and in the low frequency range they fail due to uncertainty of the resistive machine parameters for dc excitation of the stator [1]. Methods based on the tracking of saliencies using a high frequency carrier signal excitation (voltage or current) [2]-[7], or a transient pulse voltage excitation [8]-[10] have been developed over the past decade. These methods provide high bandwidth rotor position/speed and/or flux angle estimates, even at zero speed and fundamental frequency. In combination with the back-emf methods, sensorless control is now possible over the whole speed range of an AC drive. The method applied in this paper estimates the flux angle by applying test voltage pulses and calculating the leakage inductance which varies due to main path and leakage saturation [8], as well as slotting air-gap width modulation. This method is applied to a standard induction machine with skewed rotor, exhibiting a high spatial saturation effect with respect to the slotting effect. The machine saliencies will thus create both rotor and flux position-dependent modulations of similar magnitude in the resulting saliency control signal, which can be signal processed to yield the required position. In addition, there are also inter-modulation induced signal components present, which may act as disturbance and have to be approached using for example side band filter [11], or the so called structured neural network [12]. In this paper the compensation of saturation saliencies and inter-modulation effects were performed using artificial neural network (ANN) together with the necessary extraction of the rotor position signal [13] and the separation of the flux position signal component [14]. The reduction of disturbing harmonics is based on a compensation of non-ideal inverter/sensor properties and can be realized by optimization of the excitation pulses and/or placing of the sample instants [15]. There are however, specific operating states where the signal to noise ratio (SNR) of one of the extracted signal components may be deteriorated due to disturbances. When using both components for control purpose it is thus advantageous to weight each component according to its current reliability. Thus it is possible to reduce torque pulsation due to signal disturbances in these specific operating states. This weighting is especially important when using standard machines with multiple saliency and inter-modulation components. The weighting is based on specific quality indicators for each signal component.

II. TRANSIENT VOLTAGE EXCITATION METHOD

If an ac machine is operated on a voltage source inverter, it is persistently excited with short voltage pulses to enable control of the reference current. This leads to a transient change of the armature current, which is determined by the dc link voltage, the three transient phase reactances, the machines back emf, and the stator resistance.

The value of the dc link voltage can be assumed constant during the short time of the transient excitation due to the dc link capacitors. The share of the back emf and stator resistance on the current change can be eliminated by signal processing if at least two different switching states are observed. The

978-1-4244-4783-1/10/$25.00 ©2010 IEEE

transient current change is measured and the resulting signal after signal processing is thus only determined by the three transient phase reactances, which in turn are modulated during operation of the machine by different inherent saliencies [8]. This signal is denoted saliency control signal in the following.

III. Harmonic Separation and Signal Merging Scheme

The saliency control signal is a superposition of different asymmetry components and can not directly be used for sensorless control. An accurate and reliable separation of its components is essential. The separation of the different harmonic components of the saliency control signal, depicted in Fig. 1 upper diagram, is done using ANN. This separation can be used for obtaining reliable signal components for both flux- and rotor-position estimation. Full details of the technique can be found in [13] and [14]. In recent years, the ANN has found a place in real time control and system identification applications with the increase in microcontroller speed and capabilities. The ability of ANN to model nonlinear characteristics and to compensate disturbances and uncertainties makes it an ideal candidate for estimation. The structure of the ANN used in this paper is multi-layer perceptron [16]. Fig. 1 lower diagram shows the slotting component of the saliency control signal after elimination of saturation, cross-saturation effects and inter-modulation disturbance components.

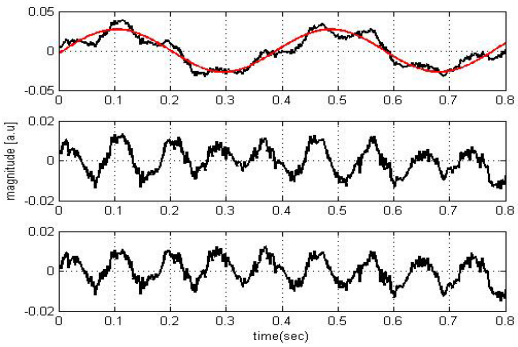

Fig. 1: Real component of saliency control signal at 90% rated load. Upper: no compensation; Middle: compensation of saturation effects; Lower: compensation of saturation effects and inter-modulation.

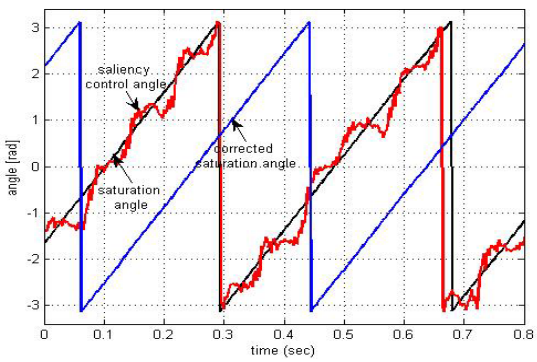

Fig. 2: Angle of saliency control signal at 90% rated load (red); estimated saturation angle (black); and corrected saturation angle (blue).

The estimated rotor position using this component is combined with the current model (rotor eq.) to get the estimated flux position [13]. Regarding the flux position estimation using the saturation saliency, Fig. 2 shows the angle of the saliency control signal before (red) and after elimination of the disturbing slotting and inter-modulation components (black). This angle is further processed using the output of an ANN (flux angle deviation) to get the corrected saturation angle (blue) that corresponds the estimated flux angle, which is the difference between saturation saliency angle and twice the flux angle obtained under sensored mode.

This angle is further processed using the fundamental wave information of the stator equation (voltage model) [14].

In order to establish an adaptive signal merging of the two estimated flux angles "$\gamma_{\psi A}$" (based on saturation signal in combination with voltage model (stator-eq.)) and "$\gamma_{\psi B}$" (based on slotting signal in combination with current model (rotor-eq.)), it is necessary to realize some sort of quality indicator for each of the signal components as in Fig. 3. This is done by comparing the instantaneous values of signal magnitude and angle of slotting and saturation signals as shown in Fig. 4. The slotting signal magnitude and angle are shown in the two upper most traces and saturation magnitude and angle in the two lower traces in Fig. 4 at 90% rated load for a standard induction machine with skewed rotor. It is shown that at time instant t=3.6 sec there is one missed slot when considering only the slotting signal. In this case the signal merging will increase the influence of the saturation signal. The quality indicator of the slotting and saturation signal in combination with the signal merging are used to determine the reliabilities of each of the flux angles "γ_{ψ}" calculated by stator and rotor equation. The most reliable one is finally used for field oriented control (FOC) as depicted in Fig. 3.

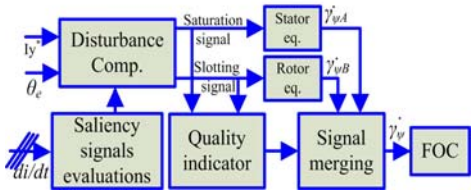

Fig. 3: Disturbances compensation and signals merging scheme.

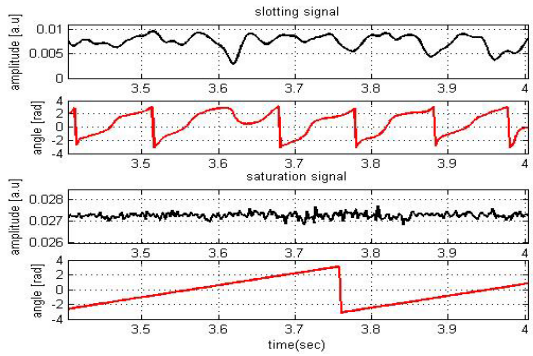

Fig. 4: From top to bottom: slotting magnitude and angle; saturation magnitude and angle at 90% rated load. (operation with 15rpm speed)

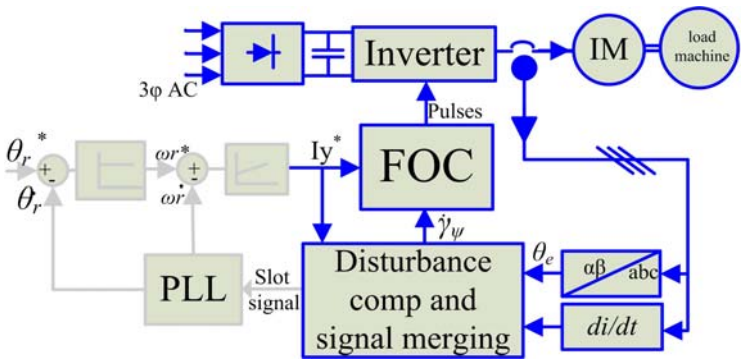

Fig. 5: Sensorless control scheme

IV. Sensorless Controlled Drive

Figure 5 shows the sensorless controlled drive using both saliencies and the proposed signals merging scheme. The individual signals disturbances are identified using ANN. The slotting signal in combination with the phase locked loop (PLL) is used to estimate the rotor angle "θ_r". Depending on the quality of the slotting and the saturation signal as well as the point of operation the adaptive signal merging of the two estimated flux angles is used to combine the reliabilities of the flux angles estimated by the stator and rotor equations and eventually to reconstruct a missed slot.

This merged flux angle "γ_ψ" is finally used for sensorless (FOC) as depicted in Fig. 5. Considering the fact that the position signal is delivering only incremental information it is possible to apply even position control (indicated with gray color) to a loaded induction machine.

V. Experimental Results

The experimental results shown are from an induction machine with skewed rotor coupled to a load machine as shown in Fig. 5. The machine under test was operated under sensorless torque controlled conditions using the proposed excitation and separation algorithm. The drive speed is imposed by the speed controlled load dynamometer.

In another arrangement the machine under test is loaded at zero mechanical speed with a weighted bar to prove position control under loaded operation at standstill.

The parameters of the machine are given in appendix I. The control is done on a digital signal processor board plugged into a computer programmable in Matlab/Simulink. It performs the vector control and separation algorithm using ANN. The pulse sequences and instances of injections of the pulses are being calculated on a field programmable gate array system (FPGA) plugged into another computer using the programming language Labview. There is a communication board between the two systems for transferring and receiving data. The induction motor was fed by a voltage source inverter with PWM operating at 5kHz. Three industrial current sensors were used for the current measurements.

An optional position signal is available from an encoder with 1024 pulses resolution as a reference signal.

A. Flux Angle Estimation using Slotting Signal

The following results are taken under sensorless field oriented torque control (based on the slotting signal in combination with the current model (rotor-eq.).

Figure 6 demonstrates the accuracy of the harmonic separation during changing saturation levels due to load change. The induction machine is operated with zero mechanical speed when a load change from 50% rated load at time instant approximately t= 6 sec to 90% rated load and the load changes from 90% rated load at time instant t= 35 sec back to 50% rated load in a ramp function to avoid problems with the Shannon frequency due to the control dynamics of the coupled load machine (sampling frequency of the rotor position signal is about 500 Hz).

The upper diagram shows the reference rotor position angle from the position encoder (black) and the estimated (mechanical) rotor position using slotting signal (red). The difference between these two angles is depicted in the lower diagram (black) in degree. The phase difference between the estimated and reference position, which is about 102.5° in the lower diagram in Fig. 6, results from a zero position offset as only incremental information is contained in the slotting signal. The quality of estimated position signal and the constant phase difference is clearly seen. The control is able to accurately determine the mechanical position within a tolerance of less than ±1° mechanical.

Figure 7 shows the same operating state but for the rotor flux angles. The upper diagram in the figure shows the flux angle obtained from the current model (red) and the flux angle from the sensor- based (reference) current model (black). The signal tracks the angle of the current model, with only limited error as shown in Fig. 7 (middle diagram).

For the same measurement setup, the error between the reference flux angle and the estimated flux angle (based on the saturation signal in combination with stabilized voltage model (stator-eq.) is depicted in Fig. 7 (lower diagram) as shown the angle error here stays within a few degrees.

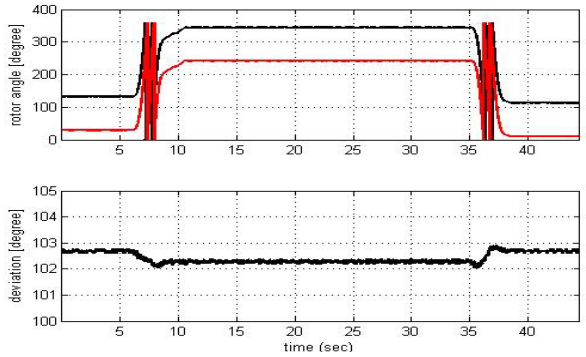

Fig. 6: Sensorless operation using current model and slotting saliency at load change from 50% to 90% rated load and from 90% to 50% rated load at standstill. Upper: Reference rotor angle (black), estimated rotor angle (red); Lower: error between reference and estimated rotor angles (°).

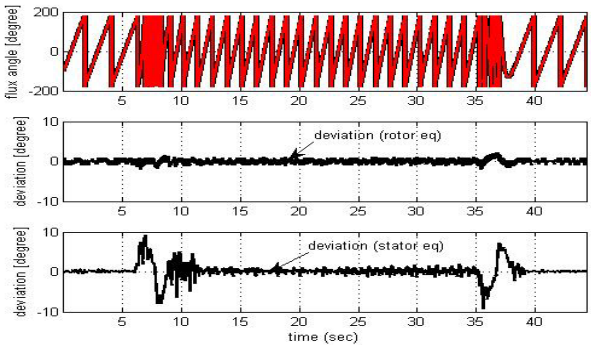

Fig. 7: Sensorless operation using current model and slotting saliency at load change from 50% to 90% rated load and from 90% to 50% rated load at standstill. Upper: Reference flux angle (sensor-based) (black), and flux angle from current model (red). Middle: error between reference and estimated angles using current model (°). Lower: error between reference and estimated angles using voltage model (°).

In Figs.8-9 the drive performs a speed reversal ±33.5 rpm under 90% rated load condition. Fig. 8 (upper diagram) shows the rotor position angle from the position encoder (black) and estimated (mechanical) rotor position using the slotting signal (red). The difference between these angles is depicted in Fig. 8 (lower diagram) in degree. At -33.5 rpm, this load condition corresponds to the drive operating around zero excitation frequency.

Since this speed equals the slip frequency at that load level, the result is zero flux frequency with a constant rotor flux position as shown in Fig. 9 (upper diagram). The upper diagram in the figure shows the flux angle obtained from the current model (red) and the flux angle from the sensor-based (reference) current model (black). The signal tracks the angle of the current model, with only limited error as shown in Fig. 9 (middle diagram).

For the same measurement setup, the error between the reference flux angle and the flux angle (based on the saturation signal in combination with stabilized voltage model (stator-eq.) is depicted in Fig. 9 (lower diagram). As was shown for the control using the rotor equation, the angle error here also stays within a few degrees.

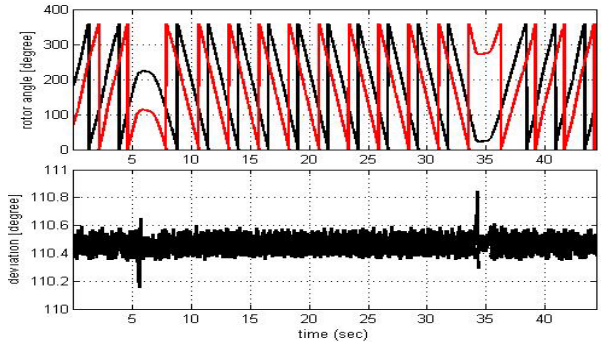

Fig. 8: Sensorless operation using current model and slotting saliency at 90% load and speed reversal ±33.5 rpm.
Upper: Reference (black) and estimated (red) rotor angle; Lower: error between reference and estimated rotor angle (°).

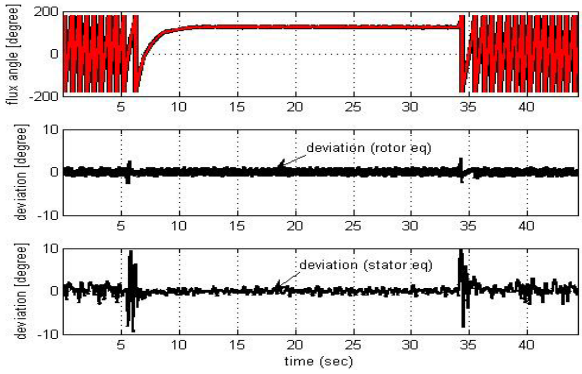

Fig. 9: Sensorless operation using current model and slotting saliency at 90% load and speed reversal ±33.5 rpm.
Upper: Reference flux angle (sensor-based) (black), and flux angle from current model (red). Middle: error between reference and estimated angles using current model (°). Lower: error between reference and estimated angles using voltage model (°).

In Fig. 8 (lower diagram) the offset value of ~110.5° again results from an initial position error as the slotting saliency component delivers only incremental information. Nevertheless the control is able to accurately determine the mechanical position within a tolerance of less than ±1.5° mechanical. The same comparison is also shown in Fig. 9 where the deviation of the estimated flux angle is approximately ±1.5° electrical. From Fig. 8 and Fig. 9 it can be seen that the tracking of the rotor speed is very accurate using the compensation technique during transient and steady state operation.

B. Flux Angle Estimation using Saturation Signal

Next results are taken under sensorless field oriented torque control (based on the saturation signal in combination with stabilized voltage model (rotor-eq.).

The induction machine is operated with zero mechanical speed when a load change from 50% rated load at time instant approximately t= 7 sec to 90% rated load and the load changes from 90% rated load at time instant t= 33 sec to 50% rated load in a ramp function to avoid problems with the Shannon frequency due to the control dynamics of the coupled load

machine. Figure 10 shows the rotor flux angles. The upper diagram in the figure shows the flux angle obtained from the voltage model (red) and the flux angle from the sensor- based (reference) current model (black). The signal tracks the angle of the current model, with only limited error as shown in Fig. 10 (middle diagram). For the same measurement setup, the error between the reference flux angle and the estimated flux angle (based on the slotting signal in combination with the current model (rotor-eq.) is depicted in Fig. 10 (lower diagram) as shown the angle error here stays within a few degrees.

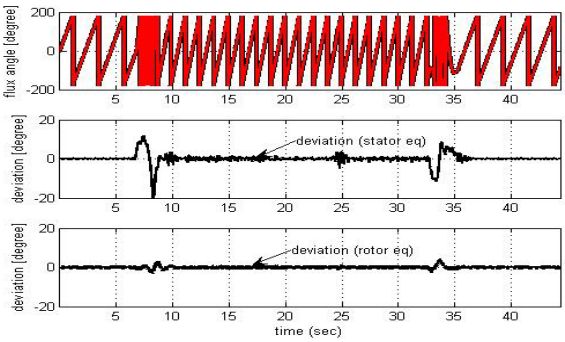

Fig. 10: Sensorless operation using voltage model and saturation saliency at load change from 50% to 90% rated load and from 90% to 50% rated load at standstill. Upper: Reference flux angle (sensor-based) (black), and flux angle from voltage model (red). Middle: error between reference and estimated angles using voltage model (°). Lower: error between reference and estimated angles using current model (°).

In Fig. 11 the drive performs a speed reversal ±33.5 rpm under 90% rated load condition. The upper diagram in the figure shows the flux angle obtained from the voltage model (red) and the flux angle from the sensor-based (reference) current model (black). The signal tracks the angle of the current model, with only limited error as shown in Fig. 11 (middle diagram). For the same measurement setup, the error between the reference flux angle and the flux angle (based on the slotting signal in combination with current model (rotor-eq.) is depicted in Fig. 11 (lower diagram). As was shown for control using the voltage equation, the angle error here also stays within a few degrees.

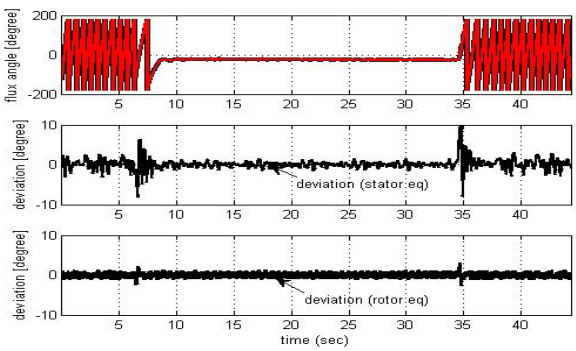

Fig. 11: Sensorless operation using voltage model and saturation saliency at 90% load and speed reversal ±33.5 rpm.
Upper: Reference flux angle (sensor-based) (black), and flux angle from voltage model (red). Middle: error between reference and estimated angles using voltage model (°). Lower: error between reference and estimated angles using current model (°).

C. *Sensorless Position Control*

Figure 12 shows the dynamic behavior of sensorless position control at no load with a change in the reference position of ±150°. The deviation between actual and estimated rotor position is about 1° mechanical during a transient position change and zero in steady state as shown in the lower diagram.

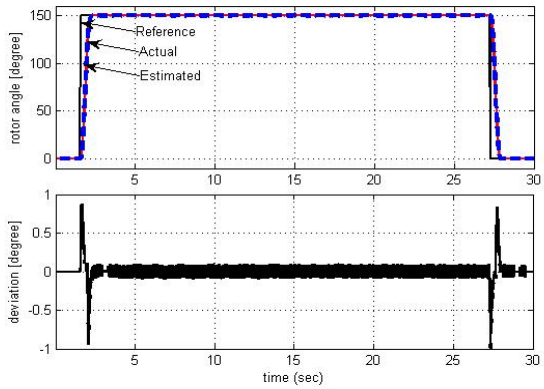

Fig. 12: Sensorless position control using current model and slotting saliency at no load and change in reference position of ±150°.
Upper: Reference rotor angle (black), estimated rotor angle (blue), and actual rotor angle (red); Lower: error between actual and estimated rotor angles in (°).

Figure 13 shows the dynamic behavior of the sensorless position control at 60% static load using a bar with load weight fixed to the rotor.

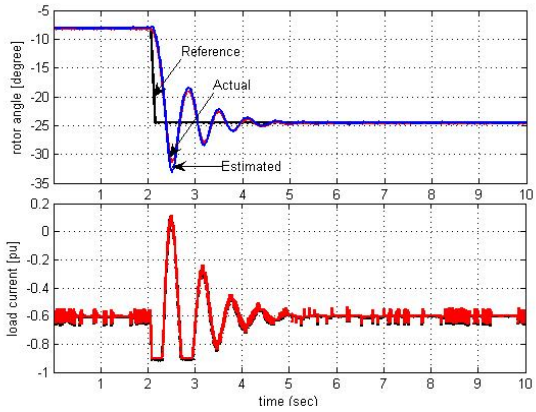

Fig. 13: Sensorless position control using current model and slotting saliency at 60% rated load and change in reference position from -8 to -24°.
Upper: Reference rotor angle (black), estimated rotor angle (blue), and actual rotor angle (red) at 60% static load; Lower: load current (p.u.).

The weight is balanced by the position control with a transient change of the reference position from -8 to -24 mechanical degrees (lifting the bar in negative direction). The deviation between actual and estimated rotor position is below ±1.5°. The response time is limited by the bandwidth of the speed controller. The position controller is proportional only. Good performance of the system is achieved noting the current controller limitation to about 90% load current imposed by the inverter as shown in the lower diagram of Fig. 13.

It should be noted that the results presented indicate the potential of the excitation method in combination with the signal processing.

VI. CONCLUSION

This paper has shown sensorless position and torque control of an full pitched stator winding induction machine with skewed rotor using transient pulse excitation and a separation algorithm. It is based on the signals obtained from an excitation of the machine with voltage pulses. The resulting signals contain a superposition of signal components caused by all saliencies present in the machine including saturation, slotting, inter-modulation and offset signal components. By identifying actual disturbance levels of the different saliency components it is possible to always use that component with the highest reliability thus reducing torque oscillations caused by signal disturbances. The paper shows how tracking of all saliencies lead to good torque and position control of machine in the zero and low frequency range at high torque levels.

APPENDIX I

Machine parameters of the applied induction machine

Nominal Current:	30A
Nominal Voltage:	280V
Nominal Frequency:	75Hz
Rated Power:	11kW

4-poles, 36 stator teeth, skewed rotor, 44 rotor bars.

ACKNOWLEDGMENT

The authors gratefully acknowledge the financial support of the Austrian Science Foundation - “Fonds zur Förderung der wissenschaftlichen Forschung” (FWF) - under grant no. P19967-N14.

REFERENCES

[1] Holtz. J., "Sensorless Control of Induction Motor Drives," *Proceedings of the IEEE,* vol. 90, No. 8, Aug. 2002.

[2] Degner, M. W., Lorenz, R.D., “Position Estimation in Induction Machines Utilizing Rotor Bar Slot Harmonics and Carrier Frequency Signal Injection”, *IEEE Trans. on Ind. Appl*., May 2000, Vol.36, no.3, pp. 736-742.

[3] Teske, N., Asher, G.M., Sumner, M., Bradley, K.J., “Analysis and Suppression of High Frequency Inverter Modulation on Sensorless Position Controlled Induction Machine Drives”, *IEEE Trans. on Ind. Appl.*, Vol. 39, no. 1, Jan. 2003, pp. 10-18.

[4] Consoli, A., Scarcella, G., Testa, A., “A New Zero-Frequency Flux-Position Detection Approach for Direct-Field-Oriented-Control Drives”, *IEEE Trans. on Ind. Appl*., May 2000, Vol. 36, no. 3, pp.797-1004.

[5] Jansen, P.L., Premerlani, W.J., Garces, L.J., “System and Method for Sensorless Rotor Tracking of Induction Machines”, US Patent no. 6,388,420 B1, May 2002.

[6] Briz, F., Degner, M.W., Garcia, P., Lorenz, R.D.,“Comparison of Saliency Based Sensorless Control Techniques for AC Machines”, *Proc. IEEE-IAS Annual Metting*, Salt Lake City, Oct. 2003, CD-ROM.

[7] Ha, J., and Sul, S.K., “Sensorless Field Orientation Control of an Induction Machine by High Frequency Signal Injection”, *Proc. IEEE-IAS Annual Metting*, New Orleans, Oct. 1997, pp 426-432.

[8] M. Schroedl, “Sensorless Control of Ac Machines at Low Speed and Standstill Based on the INFORM Method” (1996) *Proceedings of 31st IAS Annual Meeting* San Diego, Vol1, pp.270-277.

[9] J.Holtz, H. Pan, “Elimination of Saturation Effects in Sensorless Position Controlled Induction Motors”, *Proceedings of IEEE Industry Applications Annual Meeting*, Vol3, pp.1695-1702, (2002).

[10] C. Spiteri. Staines, G.M. Asher, and M. Sumner, “Sensorless Control of Induction Machines at Zero and Low Frequency using Zero Sequence Currents*”, IEEE IAS Annual Meeting*, 2004.

[11] Q. Gao, G. M. Asher, and M. Sumner, “Sensorless Position and Speed Control of Induction Motors Using High Frequency Injection and Without Offline Precommissioning”, *IEEE Trans. on Industrial Electronics*, Oct 2007, Vol. 54 pp. 2474-2481.

[12] Pablo Garcia, Fernando Briz, Dejan Racn and Robert D. Lorenz, “Saliency Tracking-based Sensorless Control of AC Machines Using Structured Neural Networks”, *the 40th Annual Meeting of IEEE, IAS* 2005.

[13] Th.M. Wolbank, and M.K. Metwally, “Zero speed sensorless control of induction machines using rotor saliencies”, the 43rd *Annual Meeting of IEEE, IAS* 2008.

[14] Th.M. Wolbank, and M.K. Metwally, “Speed Sensorless Flux and Position Control of Induction Machines Based on Pulse Injection and Multiple Saliency Extraction”, *Proceedings of IEEE Industrial Electronics Society* (IECON 2008), pp,1403-1408.

[15] Th.M. Wolbank, and J.L. Machl, “Influence of Inverter-nonlinearity and Measurement Setup on Zero Speed Sensorless Control of AC Machines Based on Voltage Pulse Injection”, *Proceedings of IEEE Industrial Electronics Society* (IECON 2005), pp,1568-1573.

[16] Bimal K. Bose, "Neural Network Applications in Power Electronics and Motor Drives—An Introduction and Perspective," *IEEE Trans. on Industrial Electronics*, vol. 54, no. 1, pp. 14-33, Jan 2007.